

# Materials Research Express



## PAPER

# Microscopic-Stress-Induced retardation between amorphous silicon nitride and amorphous indium zinc oxide having different stresses

Nakcho Choi<sup>1,2</sup> , Taekyung Yim<sup>1</sup>, Yegeon Yoon<sup>1</sup>, Byoungcho Cheong<sup>2</sup> and MunPyo Hong<sup>2,3</sup>

<sup>1</sup> Display Research Center, Samsung Display Co. Ltd, 1 Samsung-ro Giheung-gu Yongin-si, Gyeonggi-Do 17113, Republic of Korea

<sup>2</sup> Department of Applied Physics, Korea University, 2511 Sejong-ro, Sejong-si 30019, Republic of Korea

<sup>3</sup> Stretchable Display Research Center, Korea University, 2511 Sejong-ro, Sejong, 30019, Republic of Korea

E-mail: [goodmoon@korea.ac.kr](mailto:goodmoon@korea.ac.kr)

**Keywords:** birefringence, retardation, stress, polymer-stabilized vertical alignment mode

## Abstract

It is very important to increase the contrast ratio in liquid crystal display (LCD) TV using polymer-stabilized vertical alignment (PS-VA) mode. The luminance of the black state is greatly reduced by changing the parameters of the polarizer, the color filter, and the liquid crystal. However, these have the side effect of reducing the characteristics such as the transmittance, the response time, and the viewing angle. In this paper, the luminance of the black state can be reduced by lowering the stress induced retardation at the edge of pixel electrode without changing the materials in the PS-VA mode. It has been shown for the first time that the stress difference in the heterogeneous layers such as amorphous indium zinc oxide (a-IZO) and amorphous silicon nitride (a-SiN<sub>x</sub>) can optically create birefringence in the microscopic region. By controlling the stress difference in the heterogeneous membrane, the microscopic-stress-induced retardation (MSIR) could be lowered and the contrast ratio of the PS-VA mode could be increased up to 10%.

## 1. Introduction

Amorphous silicon nitride (a-SiN<sub>x</sub>), amorphous indium zinc oxide (a-IZO), and amorphous indium tin oxide (a-ITO) are commonly used as insulators and transparent electrodes in liquid crystal display (LCD) panels because they are transparent in the visible range and have low optical retardation. Therefore, all the materials in an LCD panel, such as glasses, insulators, color filters, transparent electrodes, and alignment layers (AL), are optically isotropic and in an amorphous phase. Therefore, in the LCD panel, only the transmission of light is controlled by the change of the refractive index anisotropy according to the electric field of the liquid crystal. However, if there is a local temperature difference in a large size panel, an H-band mura or a white corners mura will be produced due to stress differences in the substrate [1]. This demonstrated that stress-induced retardation of amorphous glass can result in black light leakage on the LCD. Black light leakage is also caused by stress in a curved display. The smaller the radius of the bending curvature, the larger the local stress difference, which creates a black mura of the TV product, which results in a poor display quality [2].

In our research, we found that for an LCD panel with polymer-stabilized vertical alignment (PS-VA) mode [3–5], there is light leakage near the micro-slit patterns even in the black state, which causes a reduction of contrast ratio. We have been studying that the reason of the light leakage around the micro slit electrode. It is expected that the light leakage is attributed to the optical retardation change between the a-IZO micro-slit pattern and the a-SiN<sub>x</sub> layer. Until now there have been several studies on the stress-induced retardation in an LCD panel but they are mostly based on macroscopic analyses [1, 2]. In addition, conventional SiN<sub>x</sub> and IZO thin film researches have been conducted on optical and mechanical properties according to thin film deposition conditions [6–8], but there is not much research on the optical characteristics occurring at the interface in the correlation between heterogeneous films.

In this paper, we report a micro-patterning-induced retardation change, which causes light leakage in the black state. We performed 3D model simulations in heterogeneous layers, where the retardation change can be

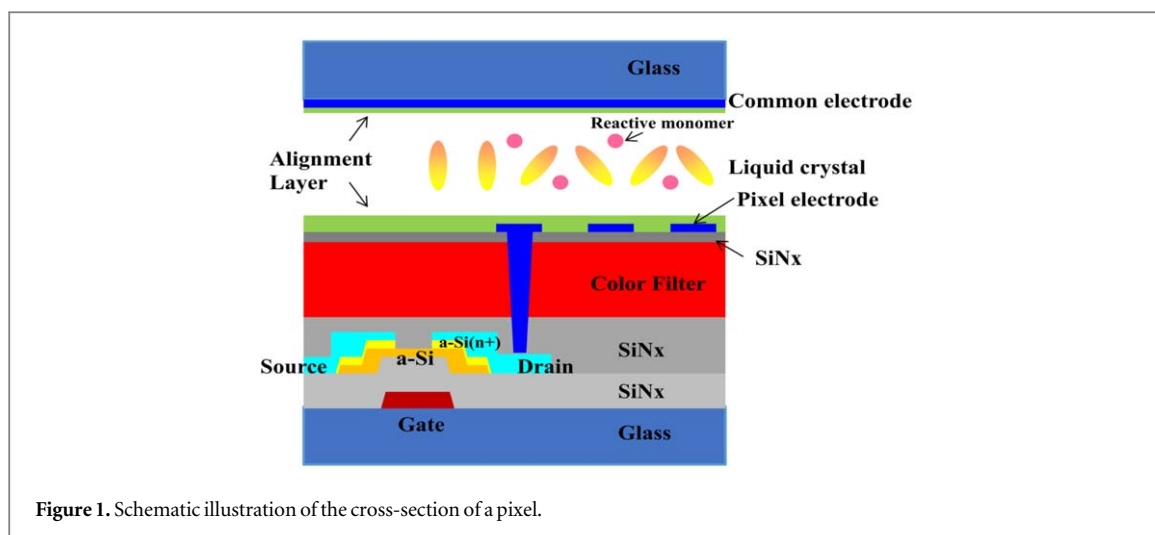


Figure 1. Schematic illustration of the cross-section of a pixel.

Table 1. Conditions of a-SiN<sub>x</sub> deposition process and stress values.

N <sub>2</sub> sccm	NH <sub>3</sub> sccm	SiH <sub>4</sub> sccm	Temperature °C	[NH <sub>3</sub> ]/[SiH <sub>4</sub> ] Υ	Stress MPa
1800	500	200	200	2.5	120
2500	800	200	200	4.0	750
3200	420	90	200	4.7	-40
3200	600	70	200	8.6	-120
3200	800	50	200	16.0	-210
2000	800	150	200	5.3	-20

made from the strain mismatch. Finally, by reducing the difference of stresses of two layer such as a-IZO and a-SiN<sub>x</sub>, We could find the solution to have a high contrast ratio without changing the materials such as polarizer, color filter, and liquid crystal.

## 2. Experimental

Figure 1 shows a schematic representation of a PS-VA LCD panel. We fabricated the back plane of the LCD using a color filter on array (COA) structure, and deposited a-SiN<sub>x</sub> with a thickness of 1000 Å as a capping layer to prevent the out gas of the color filter. Then, a-IZO was patterned on the micro slit pattern. The a-SiN<sub>x</sub> thin film deposition processes were performed at 200 °C under the process conditions shown in table 1. The source gases were SiH<sub>4</sub>, NH<sub>3</sub>, and N<sub>2</sub>; the NH<sub>3</sub>/SiH<sub>4</sub> flow ratio Υ was varied from 2.5 to 16.0 [7]. After the deposition of the a-SiN<sub>x</sub> thin film on color filter, a-IZO or a-ITO electrodes of thickness 550 Å were sputtered by direct current sputtering. The electrodes show a fishbone pattern in figure 1. The top-side glass was coated with ITO without patterning and the pair of glasses was coated with polyimide (JSR AL-60702) as ALs. The liquid crystals from Merck ( $\Delta\epsilon = -3.0$ ,  $\Delta n = 0.1$ ) were used. One-drop process was used to inject liquid crystal. This is done by dropping the liquid crystal drops between the two substrates in a vacuum, drawing the uv curable sealant on the edge of the substrate and then irradiating UV. After that, curing process was carried out at 120 °C for 1 h in order to increase the sealant hardening and to make the liquid crystal spread uniform.

The line and spacing of the micro-slit were 3 μm and 3 μm, respectively. This micro-slit pattern aligns the orientation of the liquid crystals in an applied electric vertical field parallel to the slit direction. To create the pre-tilt angle of the liquid crystals on the surface, the cell should be irradiated with UV light of energy 5 J and wavelengths 314 nm and 365 nm for 3 min while applying a driving DC voltage of 6 V to the cell. Under various deposition conditions of the a-SiN<sub>x</sub> thin film, the stress was measured using the thin film stress measurement system FSM 500TC obtained from the Institute of Materials Research and Engineering, as given in table 1. The optical retardation was measured using the image polarimeter AXO-STEP 20 H obtained from Axometrics Inc. and the pixel luminance was measured using the Imaging Photometer and Colorimeter PM-1400 camera obtained from Radiant Vision Systems.

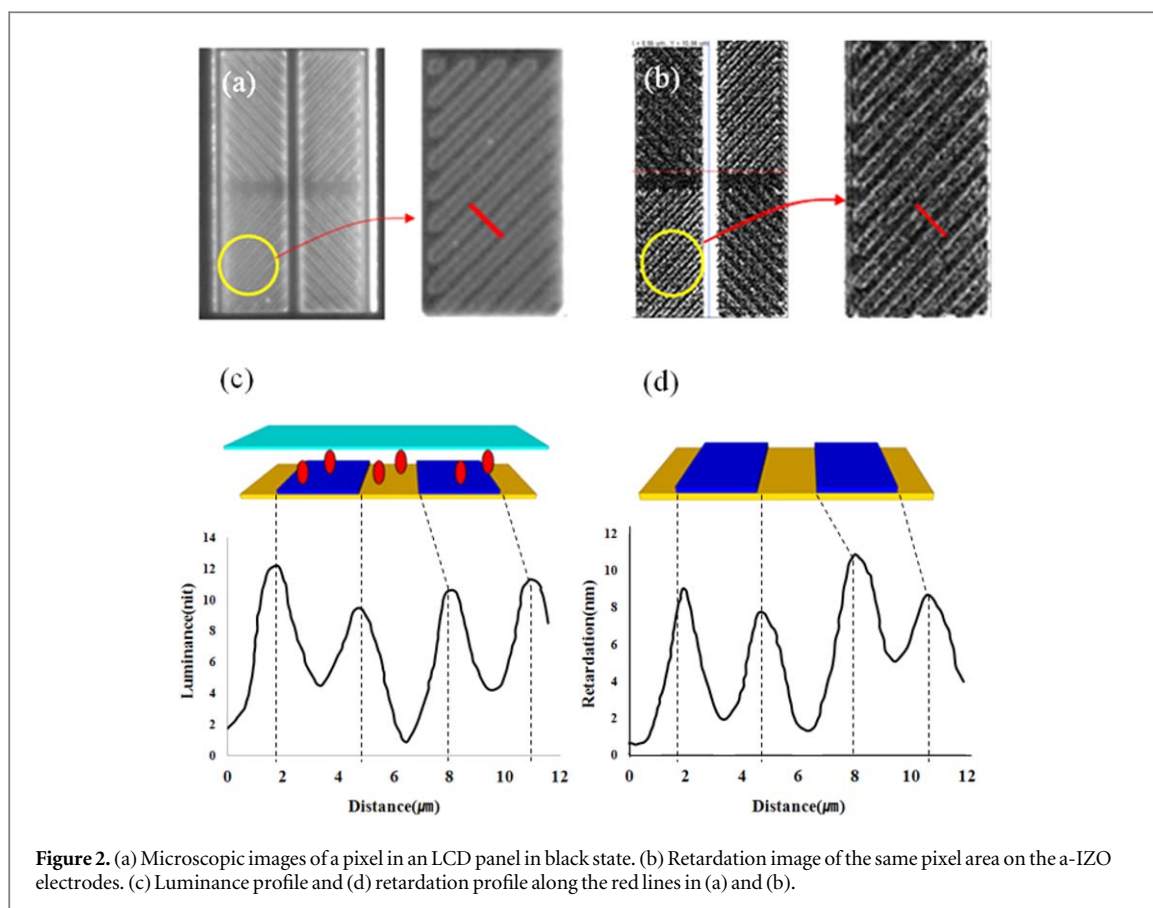


**Figure 2.** (a) Microscopic images of a pixel in an LCD panel in black state. (b) Retardation image of the same pixel area on the a-IZO electrodes. (c) Luminance profile and (d) retardation profile along the red lines in (a) and (b).

### 3. Results and discussions

#### 3.1. Measurement of light leakage and retardation

The pixel was observed using a microscope in the black state. In figure 2(a), a light leakage was strongly observed at the edge of the micro slit pixel electrode. Figure 2(c) shows a graph of the luminance change along the red line in figure 2(a). A peak of luminance is generated at the edge of the electrode, and a valley is formed at the center of the electrode or at the central portion between the electrode and the electrode.

We removed the polarizer of the LCD panel, separated the two glass plates, and removed the liquid crystal remaining on the glass plate with acetone. Then, only the lower plate glass was measured for retardation using the AXO-STEP 20 H equipment. Figure 2(b) shows the retardation image of the pixel. Similar to figure 2(a), the pixel electrode edge has a relatively high retardation value. Figure 2(d) is a graph of the retardation value measured along the red line of a micro slit electrode in figure 2(b), with a retardation peak value at the edge of the electrode. And the center of the electrode and the center of space between two electrodes have the value of the retardation.

#### 3.2. Retardations and transmittances of various electrodes and thicknesses

The retardation can be converted into the transmittance change as follows:

$$T = \frac{1}{2} \left( \sin \frac{\pi \text{Re}}{\lambda} \right)^2, \quad (1)$$

where  $T$ ,  $\text{Re}$ , and  $\lambda$  represent the luminance, retardation, and wavelength, respectively [9].

To explore the retardation changes according to the different electrode materials and different layer thicknesses, we used the three electrodes a-IZO (550 Å), a-ITO (550 Å), and a-ITO (450 Å). Then, the transmittance was calculated by substituting retardation for each case using equation (1).

Figure 3(a) shows the retardation images in 3 kinds of pixels. Compared with a-IZO, a-ITO had a low retardation value. Also, the lower the thickness of electrode, the smaller the retardation value. Then, liquid crystals were dropped on three kinds of substrates, and they were assembled with top ITO glasses. And polarizers were attached to the outside of the upper and lower glasses. Finally, the luminance of black state was measured. The bar chart values in figure 3(b) are the measured black luminance of the three panels, and the line graph values are the calculated using equation (1) for the retardation value with measured retardation in

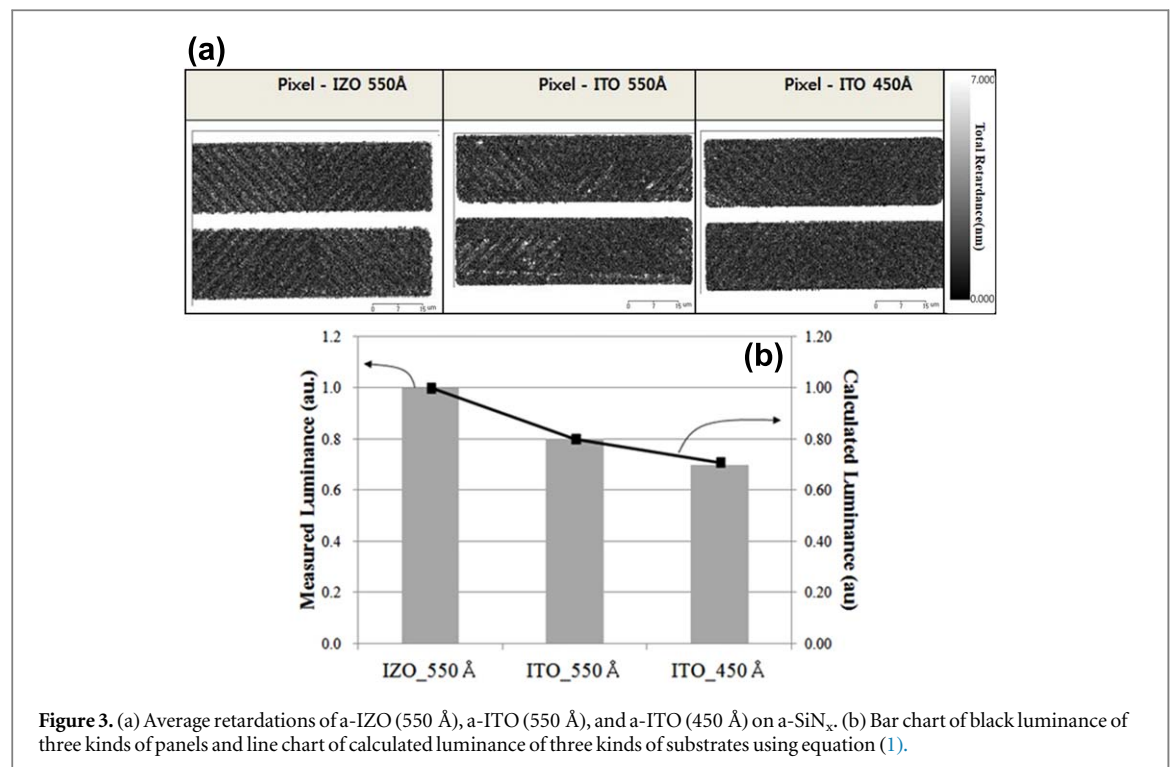


**Figure 3.** (a) Average retardations of a-IZO (550 Å), a-ITO (550 Å), and a-ITO (450 Å) on a-SiNx. (b) Bar chart of black luminance of three kinds of panels and line chart of calculated luminance of three kinds of substrates using equation (1).

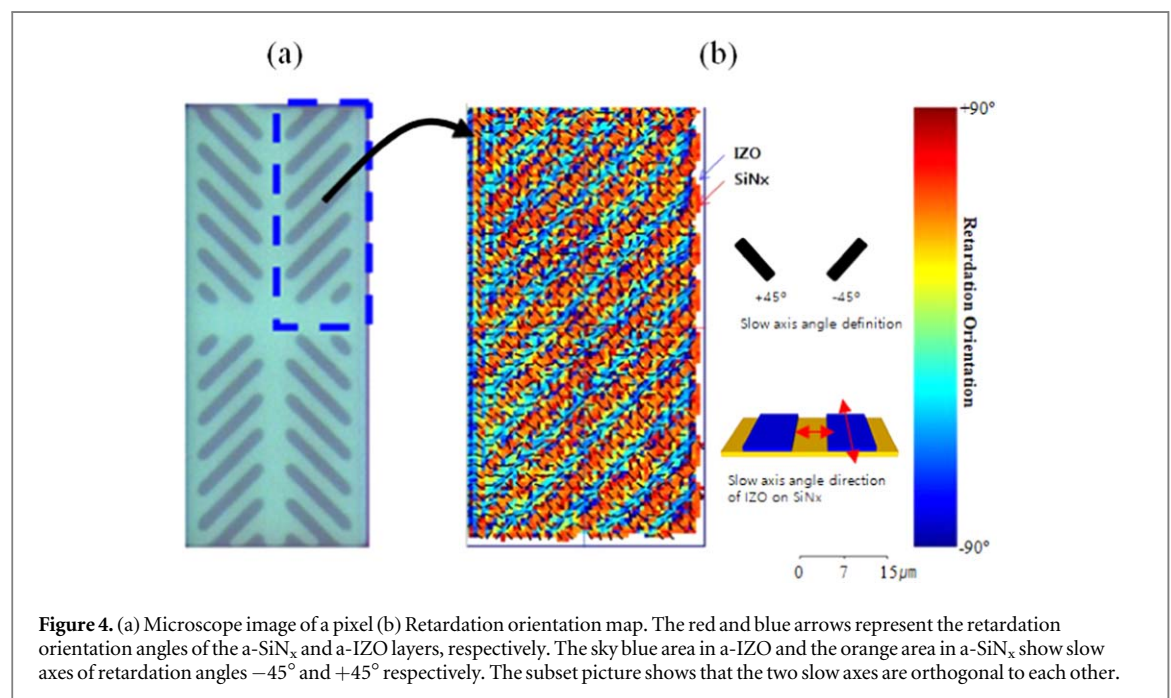


**Figure 4.** (a) Microscope image of a pixel (b) Retardation orientation map. The red and blue arrows represent the retardation orientation angles of the a-SiNx and a-IZO layers, respectively. The sky blue area in a-IZO and the orange area in a-SiNx show slow axes of retardation angles  $-45^\circ$  and  $+45^\circ$  respectively. The subset picture shows that the two slow axes are orthogonal to each other.

figure 3(a). The retardation values were obtained from each image and the average values were obtained. The values of 1.9 nm, 1.7 nm and 1.6 nm were obtained.

Figure 3(b) shows that the measured black luminance and calculated black luminance have the same trend. It means that the light leakage in the black state is related to the retardation near the edge of the slit-patterned electrodes.

Figure 4 shows (a) the pixel microscopic image and (b) the retardation orientation map. Retardation orientation refers to the direction of the optical slow axis. The direction in which the speed of light slows as the polarized light passes through a material with refractive index anisotropy is the direction of retardation orientation. Before a-IZO is patterned on the a-SiNx layer, there is no retardation and the retardation orientation has random orientation. However, when a-IZO is patterned, stress-induced retardation occurs at

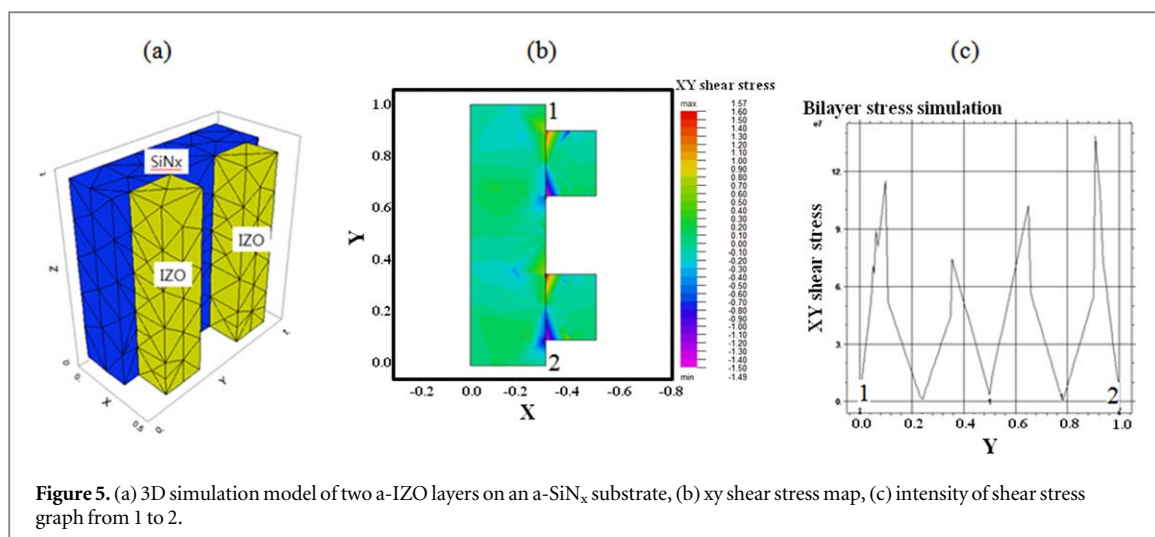


**Figure 5.** (a) 3D simulation model of two a-IZO layers on an a-SiNx substrate, (b) xy shear stress map, (c) intensity of shear stress graph from 1 to 2.

**Table 2.** Simulation conditions (FlexPDE).

	Thermal conductivity [ $\text{W m}^{-1} \text{K}^{-1}$ ]	Young's modulus [GPa]	Expansion coefficient [ $^{\circ}\text{C}^{-1}$ ]	Poisson's ratio
IZO	1.2	141	$24.8 \times 10^{-6}$	0.25
SiNx	16	160	$3.27 \times 10^{-6}$	0.253

the pattern boundary due to local stress relaxation, and the retardation orientation is measured perpendicular to the boundary.

In figure 4(b), the electrode and space regions are red and sky blue, which means that the slow axis directions are  $-45^{\circ}$ ,  $+45^{\circ}$ , and perpendicular to each other.

To explain the origin of the inhomogeneous retardation orientation, we propose a ‘microscopic-stress-induced retardation (MSIR) model’ for the double-layered amorphous materials. The release of stress locally can induce retardation change near the border of the two amorphous layers. The direction of the stresses at the top and bottom layers can be perpendicular owing to the Poisson effect [10]. When an amorphous layer is compressed in one direction, it tends to expand in the other two orthogonal directions. Thus, in a heterogeneous system composed of amorphous materials, the top and bottom surfaces have the orthogonality of the slow axes during the patterning process of the top a-IZO layer. Stress-induced retardation occurs on a microscopic scale as given in equation (2).

$$\text{Re} = \frac{2\pi t}{\lambda} C(S_1 - S_2), \quad (2)$$

where Re, C, t, and  $S_1$  and  $S_2$  represent the induced retardation, stress-optic coefficient, thickness, and the first and second principle stresses, respectively.

### 3.3. Stress simulation on the patterned bi-layers

To verify the existence of MSIR, we performed a numerical simulation using the FlexPDE code given by PDE Solutions Inc. [11]. A simple model composed of two plates on a flat substrate is constructed as shown in figure 5(a), where we used different heat expansion coefficients and Poisson ratios in a-IZO and a-SiNx, as listed in table 2 [12–14]. As a result of the simulation, it was found that the shear stress was concentrated at the boundary of the a-IZO pattern as shown in figure 5(b). Figure 5(c) shows the stress intensity distribution from position 1 to position 2, which has a similar tendency to the retardation graph in figure 5(b). From this simulation, it is observed that the shear stress is the highest at the edge of a-IZO on a-SiNx, which is consistent with the measurement results.

Figure 6 shows the shear stress map according to various stresses of the a-IZO and a-SiNx thin films, where we could find that the shear stress can be minimized when the top and bottom layers have the same stress behaviors (tensile/tensile or compressive/compressive).

From the simulation results, it can be explained that the shear stress leads to retardation, as given in equation (2), which is the main cause of light leakage near the edge of the micro-slit pattern in the black state of the PS-VA panel in figure 2.



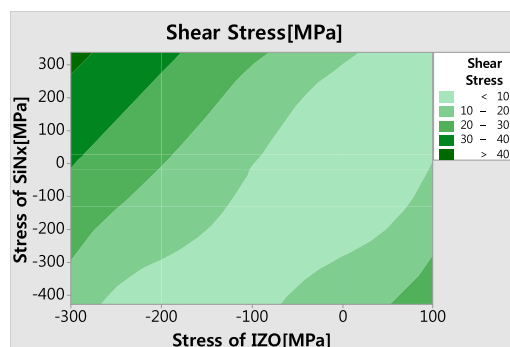


Figure 6. Simulation results of shear stress map for stress combinations between a-IZO and a-SiN<sub>x</sub>.

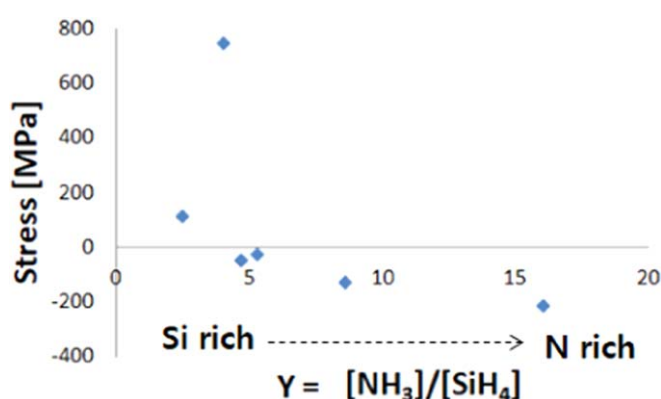


Figure 7. Stresses of a-SiN<sub>x</sub> according to  $\Upsilon$  [NH<sub>3</sub>]/[SiH<sub>4</sub>].

### 3.4. Verification experiment of minimization of contrast ratio in mass production line

To minimize MSIR, the stress values of the a-SiN<sub>x</sub> layer in the LCD panels were manipulated by controlling the a-SiN<sub>x</sub> deposition processes as indicated in table 1. In figure 7, Si rich SiN<sub>x</sub> has tensile stress and N rich SiN<sub>x</sub> has compress stress. By defining  $\Upsilon$  as [NH<sub>3</sub>]/[SiH<sub>4</sub>] and measuring the stress of a-SiN<sub>x</sub> according to gamma value, an inverse curve can be obtained.

After patterning a-IZO on 4 kinds of a-SiN<sub>x</sub> substrates with different stress values, 6 points of retardation were measured respectively and then plotted in box plot in figure 8. The stress of a-IZO was measured at 27 MPa and the stresses of a-SiN<sub>x</sub> were measured at -378, 212, 346 and 486 Mpa, respectively.

In the simulated graph of figure 6, it is predicted that when the stresses of a-IZO and a-SiN<sub>x</sub> are similar, the minimum shear stress and the MSIP also have the minimum value. As shown in figure 8, when the stress of a-IZO is fixed at 27 MPa, the stress of a-SiN<sub>x</sub> has the minimum value of MSIP at 212 MPa. However, it can be assumed that a point smaller than 212 may have a minimum value because the a-SiN<sub>x</sub> value is not finely split evaluated. Nonetheless, my assumption that the MSIP is caused by the difference in stresses of the heterogeneous layers and can be minimized when the stress values of the two layers are similar can be proved in figure 8.

In order to experimentally demonstrate that the contrast of the LCD product can be increased by minimizing the brightness of black when the MSIR is minimized, this time experiment was conducted by changing the a-IZO deposition condition. We changed the stress of the a-IZO thin film by controlling the sputtering power and pressure, as shown in table 3. After performing the micro-slit patterning process of the a-IZO electrode on the same of a-SiN<sub>x</sub>, we measured the bar and space length in the micro-slits and observed that all samples had the same slit lengths. Because if the slit design is changed as the a-IZO condition is changed, the contrast ratio cannot be accurately compared. The measured retardation images and the contrast ratio of the three LCD panels are shown in figures 9(a) and (b). We made more than 40 panels in IZO\_1 and IZO\_2 conditions respectively, and measured the contrast ratio and got the average value. Figure 9(a) shows that the IZO\_2 layer has a lower retardation value, which indicates that the MSIR could be minimized. Furthermore, the minimum retardation panel produces a higher contrast ratio. It is observed that the contrast ratio of IZO\_2 is 4774, which is approximately 10% larger than that of the reference panel with 4317.

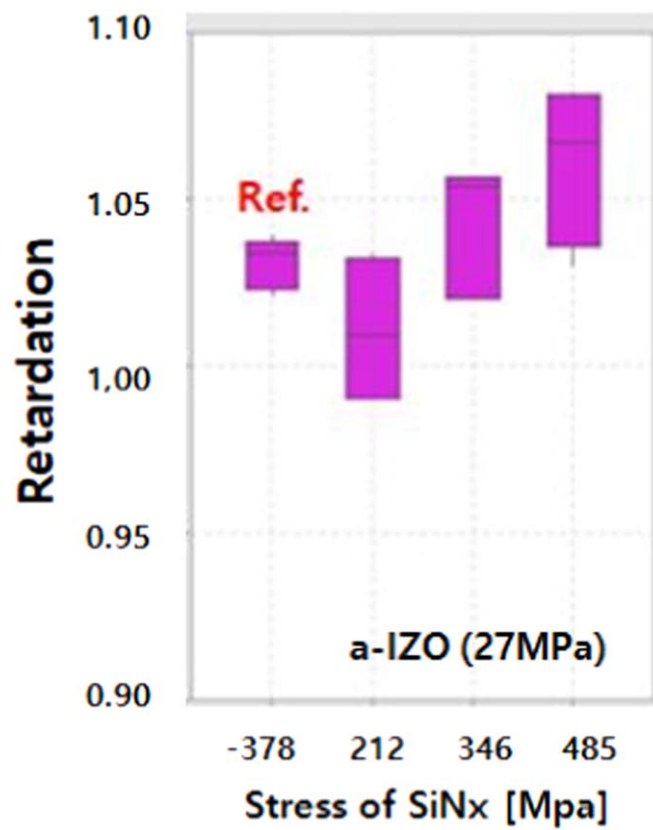


Figure 8. Retardations of patterned a-IZO on a-SiNx with 4 kinds of stresses.

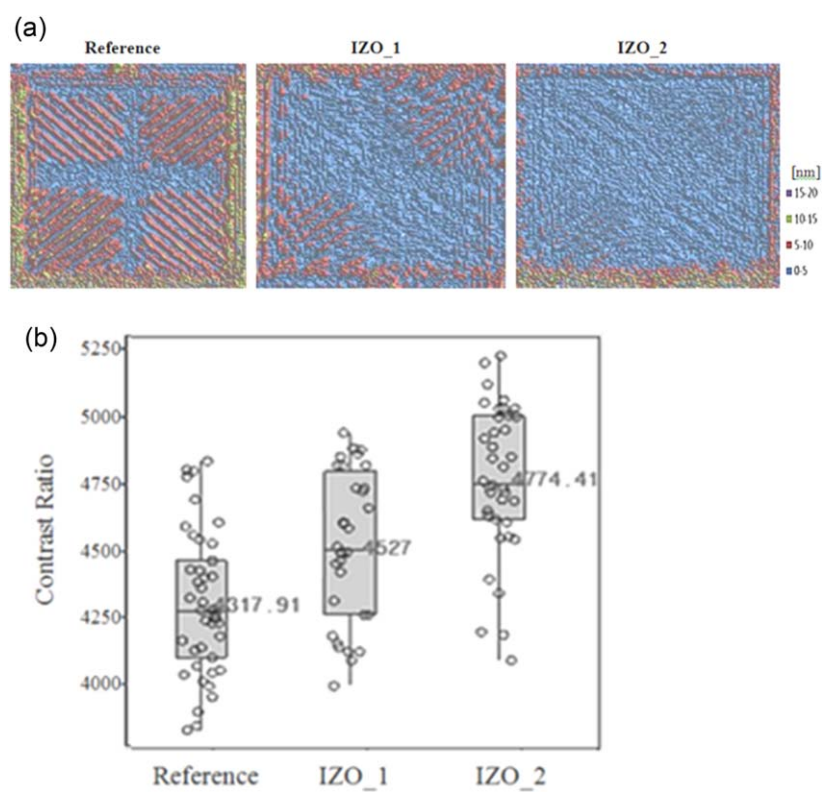


Figure 9. (a) Retardation images of 3 kinds of IZO electrodes (b) Contrast ratio of 3 kinds of panels with different stress of IZO.

**Table 3.** Experimental conditions for IZO.

Material Condition	IZO		SiN <sub>x</sub>	
	Power	Pressure	Power	Pressure
Reference	13 kW	0.55 Pa	11.5 kW	0.11 Pa
IZO_1	13 kW	0.35 Pa	11.5 kW	0.11 Pa
IZO_2	8 kW	0.55 Pa	11.5 kW	0.11 Pa

## 4. Conclusions

We proposed that MSIR occurred near the edge of the micrometer-scaled electrode patterns in a bi-layer system composed of amorphous thin films with opposite stress behaviors. This was able to measure the black luminance and retardation images very precisely at the micrometer-scale level, so we could connect the interrelationships. We have found that the physical phenomenon of stress-induced birefringence can occur in the patterning process, and this is one of the causes of the increase in the luminance of the black state in PS-VA mode. To reduce the stress mismatch between the two amorphous layers, we optimized the deposition process of the a-IZO and/or the a-SiN<sub>x</sub> thin films and minimized the retardation value, achieving a higher contrast ratio up to 10%. By applying the specifically optimized conditions on the amorphous bi-layers (slit-patterned electrode/dielectric) in the PS-VA LCD panels, the reduction of the contrast ratio caused by MSIR would be eliminated effectively.

## Acknowledgments

This research was supported by Basic Science Research Program through the National Research Foundation of Korea(NRF) funded by the Ministry of Education(2014R1A6A103073). This work was supported by ‘Human Resources Program in Energy Technology’ of the Korea Institute of Energy Technology Evaluation and Planning (KETEP), granted financial resource from the Ministry of Trade, Industry & Energy, Republic of Korea (No. 20184030201910).

## ORCID iDs

Nakcho Choi  <https://orcid.org/0000-0001-7176-9595>

## References

- [1] Greene R G *et al* 2011 *SID 2005 DIGEST* **42** 655
- [2] Vepakomma V H *et al* 2015 *SID 2015 DIGEST* **46** 634
- [3] Hanaoka K *et al* 2004 *SID 2004 DIGEST* **35** 1200
- [4] Kim S G *et al* 2007 *Applied Physics Letters* **90** 261910
- [5] Kim S M *et al* 2009 *Japanese Journal of Applied Physics* **48** 032405
- [6] Gan Z *et al* 2018 *Surface* **1** 59
- [7] Masaki Y *et al* 1993 *Journal OF Applied Physics* **75** 5088
- [8] Ito N *et al* 2006 *Thin Solid Films* **496** 99
- [9] PochiYeh C G 2006 *Optics of Liquid Crystal Displays* (New York, USA: Wiley) 118
- [10] Gercek H *et al* 2007 *International Journal of Rock Mechanics and Mining Sciences* **44** 1
- [11] 2002 *User Manual: FlexPDE* (Antioch, CA: PDE Solutions, Inc.)
- [12] Endoh R *et al* 2011 *MRS Proceedings* **1315** 125
- [13] Zeng K *et al* 2003 *Thin Solid Film* **443** 60
- [14] Tien C L *et al* 2012 *Applied Optics* **51** 7229